Paramagnetic susceptibility simulations from crystal-field effects on rare-earth double molybdate and tungstate $Na_5RE(XO_4)_4$

1996 J. Phys.: Condens. Matter 8 6413

(http://iopscience.iop.org/0953-8984/8/35/010)

J. Phys.: Condens. Matter **8** (1996) 6413–6424. Printed in the UK

Paramagnetic susceptibility simulations from crystal-field effects on rare-earth double molybdate and tungstate $Na_5RE(XO_4)_4$

C Cascales†‖, P Porcher‡ and R Sáez-Puche§

† Instituto de Ciencia de Materiales de Madrid, CSIC, Cantoblanco, E-28049 Madrid, Spain
‡ Laboratoire de Chimie Métallurgique et Spectroscopie des Terres Rares, UPR 209 CNRS 1, Place A Briand, F-92195 Meudon, France
§ Departamento de Química Inorgánica, Facultad de Ciencias Químicas, Universidad Complutense de Madrid, E-28040 Madrid, Spain

Received 28 February 1996, in final form 29 April 1996

Abstract. Magnetic susceptibilities of polycrystalline samples of two series of double rare-earth molybdate and tungstate compounds, $Na_5RE(XO_4)_4$ (RE = rare earth, X = Mo or W), with scheelite-type structure, space group $I4_1/a$ (No 88), where RE atoms adopt S_4 point symmetry, have been measured in the temperature range 1.7–400 K. Using the wavefunctions and energy levels derived from standard free-ion and crystal-field parameters deduced from the analysis of the optical spectra of some selected (Pr, Nd and Eu) compounds, a systematic calculation of the temperature-dependent paramagnetic susceptibility, for all $4f^N$ rare-earth configurations on the two series, has been carried out according to the Van Vleck formula. Very good agreements with experimental data are found over the whole temperature range. The standard crystal-field treatment of $4f^N$ ions is shown to explain the magnetic properties of these compounds, for which no kind of magnetic interaction among the rare-earth ions has been detected.

1. Introduction

The conventional, phenomenological description of the crystal field is a well-proven tool for the interpretation of spectroscopic, magnetic and other physical properties of solids. In this way, the use of complete free-atom and crystal-field Hamiltonians of the $4f^N$ configurations yields wavefunctions from which the paramagnetic susceptibility for any crystallographic direction and its temperature dependence as well as the g-values can be computed when the same $\boldsymbol{L} + \mathbf{g}_e\boldsymbol{S}$ tensorial operator is applied to the wavefunction of a level.

In previous works [1–3] two of the authors reported a detailed spectroscopic study on the molybdate series for the $4f^2$, $4f^3$ and $4f^6$ configurations of Pr^{3+}, Nd^{3+} and Eu^{3+}, respectively. From experimental data consisting of absorption and emission measurements between liquid-helium and room temperatures, nearly complete energy level schemes were derived, showing very good correlations between the experimental and simulated energy levels, for the approximated D_{2d} and then for the true S_4 symmetries of the rare-earth position. In fact, for the present S_4 point symmetry, the crystal-field potential involves a quite reduced number of crystal-field parameters (cfps): only five real and two imaginary cfps. Complete sets of those cfps as well as free-ion parameters have been reported for

‖ Author to whom any correspondence should be addressed.

0953-8984/96/356413+12$19.50

the above-mentioned compounds, and they were found to vary smoothly with the atomic number of the rare earth.

In the present work we show the results of the methodical comparison of the observed magnetic susceptibility with calculated curves derived from wavefunctions generated through phenomenological and/or calculated cfps, for both molybdate and tungstate $Na_5RE(XO_4)_4$ series. That comparison constitutes an excellent opportunity to test the ability of the crystal-field model to give 'correct' wavefunctions for an ion under consideration.

2. Experimental details

Polycrystalline $Na_5RE(XO_4)_4$ samples were prepared by solid-state reactions using stoichiometric amounts of 99.9% pure rare-earth sesquioxides, Na_2CO_3 and MoO_3 or WO_3 as starting materials, with final heat treatments at 530 and 600 °C for X = Mo and W, respectively. Sample purity and crystal structure were tested by x-ray diffraction analysis.

Optical measurements of some pure (R = Pr, Nd) or doped (5%-Eu-activated $Na_5Gd(XO_4)_4$) compounds have been previously reported [1, 2]. A SQUID (Quantum Design) magnetometer operating from 400 to 1.7 K at 5000 Oe was used to perform the dc magnetic measurements. The diamagnetic corrections introduced were calculated using the standard [4] values (in -1×10^{-6} emu mol^{-1}) of 5 for Na^+; 17 for Lu^{3+}; 18 for Er^{3+}, Tm^{3+} and Yb^{3+}; 19 for Dy^{3+} and Ho^{3+}; 20 for Eu^{3+}, Gd^{3+}, Nd^{3+}, Pr^{3+} and Sm^{3+}; and estimated values of 55 and 60 for the XO_4^{2-} groups, molybdate and tungstate, respectively.

3. Crystal-field analysis and simulation of the energy level schemes

In the development of a complete Hamiltonian for $4f^N$ configurations, the central-field approximation allows one to consider separately the Hamiltonians corresponding to the gaseous free-ion and to the crystal-field interactions which arise when the ion is in a condensed phase. Then the Hamiltonian consists of two parts:

$$\mathcal{H} = H_{\mathrm{FI}} + H_{\mathrm{CF}}.$$

The interactions primarily responsible for the free-ion structure can be written as

$$H_{\mathrm{FI}} = H_0 + \sum_{k=0,1,2,3} E_k e^k + \zeta_{4\mathrm{f}} A_{\mathrm{SO}} + \alpha L(L+1) + \beta G(G_2) + \gamma G(R_7) + \sum_{k=2,3,4,6,7,8} T^k t_k$$

where H_0 is the spherically symmetric one-electron term of the Hamiltonian; E_k and $\zeta_{4\mathrm{f}}$ are the Racah parameters and the spin–orbit coupling constant, and e^k and A_{SO} represent the angular parts of the electrostatic repulsion and spin–orbit coupling, respectively. For the configurations of two or more equivalent electrons the two-body interactions are considered with Tree's parameters α, β and γ associated with Casimir operators $G(G_2)$ and $G(R_7)$. For configurations having more than two electrons, non-negligible three-body interactions can also be introduced (T^γ-parameters). We do not consider here the spin–spin, spin–other-orbit and other relativistic interactions of minor importance which could be simulated through the P^k-integrals ($k = 2, 4, 6$) and Marvin M_k-integrals ($k = 0, 2, 4$).

The crystal-field calculations are usually carried out within the single-particle crystal-field theory. Following Wybourne's formalism [5], the crystal-field Hamiltonian is expressed

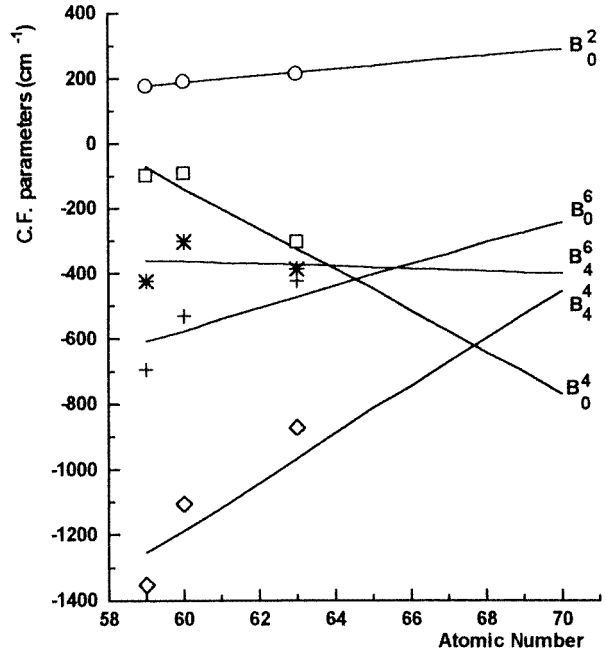

(a)

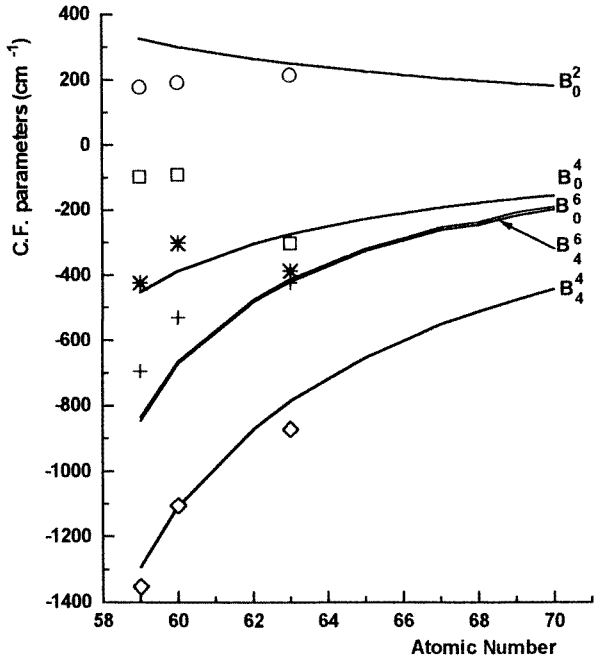

(b)

Figure 1. Experimental versus (a) extrapolated cfps (top) and (b) cfps calculated using the SOM (bottom) for the $Na_5RE(MoO_4)_4$ series.

as a sum of products of spherical harmonics and crystal-field parameters:

$$H_{\mathrm{CF}} = \sum_{k=2}^{4,6} \sum_{q=0}^{k} \left[B_q^k (C_q^k + (-1)^q C_{-q}^k) + \mathrm{i} S_q^k (C_q^k - (-1)^q C_{-q}^k) \right].$$

The number of the non-zero B_q^k and S_q^k phenomenological cfps depends on the crystallographic point-site symmetry of the lanthanide ion. When the S_4 symmetry is considered for RE in $Na_5RE(XO_4)_4$ the crystal-field potential involves five real B_q^k- and two imaginary S_q^k-parameters, immediately reduced to six parameters by an appropriate choice of the reference axis system, which cancels S_4^4. When the symmetry is approximated to D_{2d}, all of the S_q^k vanish. The fitting procedure between experimental and calculated energy level values was conducted by minimizing the root mean square (r.m.s.) deviation, chosen as the factor of merit. Schemes of 35, 76 and 21 energy levels were considered in simulations for Pr, Nd and Eu molybdate materials, respectively. Very good correlations were obtained between experimental transition energies and the computed level structures [2].

4. *A priori* calculation of crystal-field parameters: the simple overlap model (SOM)

Among all of the reported *a priori* calculation models of the cfps [6–11], recently revised and examined by one of the authors [12, 13], that known as the simple overlap model, SOM [11], has been chosen to be applied in this case. Only the first coordination sphere around the rare-earth cation is retained, i.e., the required crystallographic position data are restricted to the closest ligand positions. The covalence is represented by the overlap ρ between the rare-earth and the ligand orbitals. The cfps are written as

$$B_q^k = \rho \left(\frac{2}{1 \pm \rho} \right)^{k+1} \langle r^k \rangle A_q^k$$

with

$$\rho = \rho_0 \left(\frac{R_0}{R} \right)^n.$$

In the expression for B_q^k the radial integral $\langle r^k \rangle$ is not corrected from the spatial expansion because only the first neighbours are considered. The lattice sums A_q^k are calculated with an effective charge for the ligand. The $\pm$ sign in the denominator is present to differentiate the type of ligand, the $-$ sign being for the most covalent. The overlap ρ varies for each ligand as a function of the distance from the central ion and is referred to the closest ligand. Thus, this model involves only three adjustable parameters: the overlap, the effective charge and n, the exponent of the overlap variation with the distance. In order to normalize the curves calculated using the SOM to the experimental ones (first for $Na_5Eu(MoO_4)_4$, then for Pr and Nd compounds), a comparison of calculated and observed strength parameters was made for the three cases. The strength parameter is defined [14] in terms of the cfps as follows:

$$S = \left\{ (1/3) \sum_k [1/(2k+1)] \left[(B_0^k)^2 + 2 \sum_{kq} [(B_q^k)^2 + (S_q^k)^2] \right] \right\}^{1/2}$$

which is a quantitative measure of the strength of the crystal-field interaction of a particular rare-earth ion in a particular host. In these comparisons n was fixed at 3.5, a value of -0.8 was taken as the effective charge for oxygen—a value which is found not to vary much [15]—and the overlap ρ, ranging for $4f^N$ configurations from 0.04 (mostly ionic

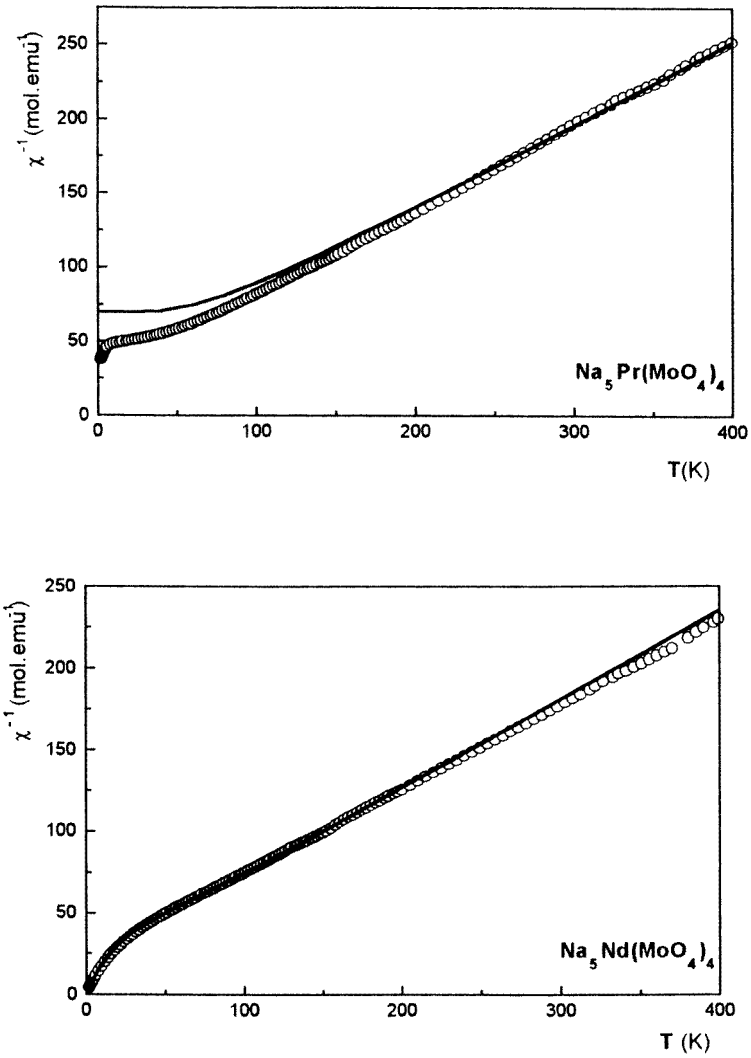

Figure 2. The temperature variation of the experimental (symbols) and calculated (solid lines) χ^{-1} (or χ for the Eu^{3+} compound) for $Na_5RE(MoO_4)_4$ materials. The cfps are those from figure 1(a).

compounds) to 0.08 (mostly covalent compounds), was finally adjusted to an intermediate value, 0.05, which was utilized for all compounds, for the molybdate as well as the tungstate series. Crystallographic data were taken from [16, 17].

5. Magnetic susceptibility and crystal-field levels

The calculation of the magnetic susceptibility of these rare-earth compounds has been carried out from the consistent sets of wavefunctions and energy levels previously determined by diagonalizing the above-mentioned crystal-field Hamiltonian. This is done here using the

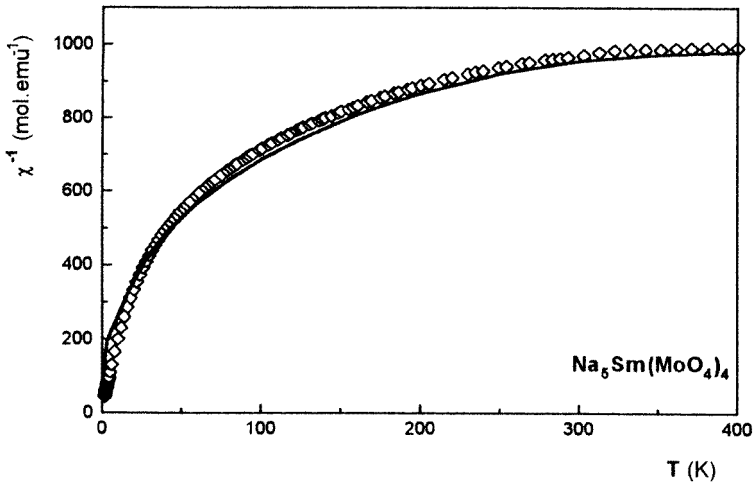

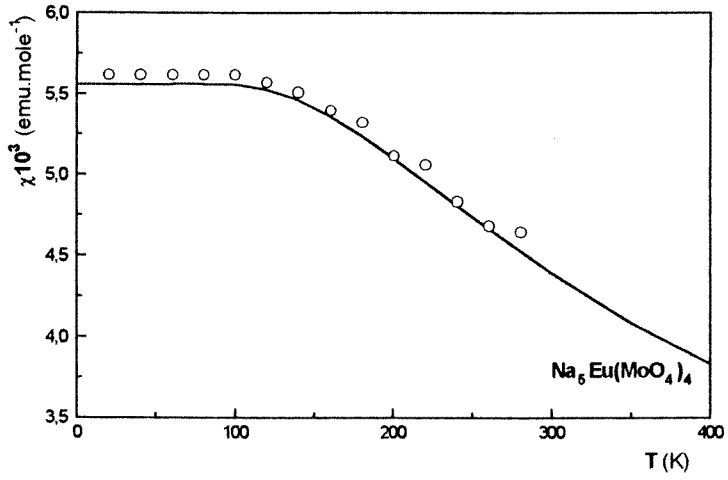

Figure 2. (Continued)

Van Vleck formula [18, 19]:

$$\chi = N\beta^2 \sum_i \left[\frac{(\varepsilon_i^{(1)})^2}{kT} - 2\varepsilon_i^{(2)} \right] \exp -\left(\frac{E_i^{(0)}}{kT}\right) \Big/ \sum_i \exp -\left(\frac{E_i^{(0)}}{kT}\right)$$

with

$$\varepsilon_i^{(1)} = \langle \Psi_i^{(0)} | (\boldsymbol{L} + \mathbf{g}_e \boldsymbol{S}) \cdot \boldsymbol{u} | \Psi_i^{(0)} \rangle$$

and

$$\varepsilon_i^{(2)} = \sum_{E_i^{(0)} \neq E_j^{(0)}}^{j} \frac{\left[\langle \Psi_i^{(0)} | (\boldsymbol{L} + g_e \boldsymbol{S}) \cdot \boldsymbol{u} | \Psi_j^{(0)} \rangle \right]^2}{E_i^{(0)} - E_j^{(0)}}$$

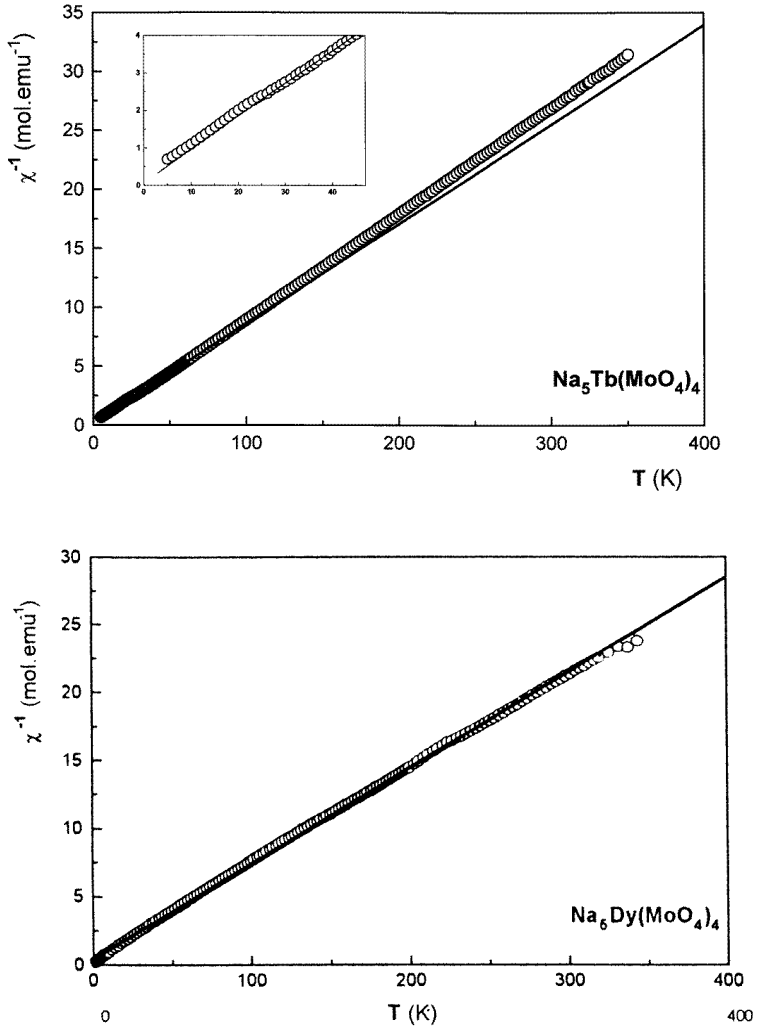

Figure 2. (Continued)

in which N is Avogadro's number, β the Bohr magneton, k the Boltzmann constant, E and Ψ the non-perturbed eigenvalues and wavefunctions, respectively, described on the $|SLJM_J\rangle$ basis, and the magnetic dipole operator $\boldsymbol{L} + g_e\boldsymbol{S}$, is represented by a tensor of rank 1. The diamagnetic second-order Zeeman term has been neglected in this expression for the paramagnetic susceptibility. The sum runs over all other states ($b \neq a$). The different values of the tensor components (or combinations of them) destroy the isotropy observed for the free ion or even for an ion in a cubic symmetry. The anisotropic components are denoted as $\chi_\perp$ (the ± 1 component of the tensor) and $\chi_\parallel$ (the 0 component of the tensor). For polycrystalline samples, the average paramagnetic susceptibility is $\chi_{av} = (2\chi_\perp + \chi_\parallel)/3$. The sum runs over all thermally populated levels, according to the Boltzmann population. In the expression, the matrix elements are calculated using the Racah algebra rules.

Other than for Eu^{3+} compounds, and to lesser extent for Sm^{3+} compounds, the diagonal

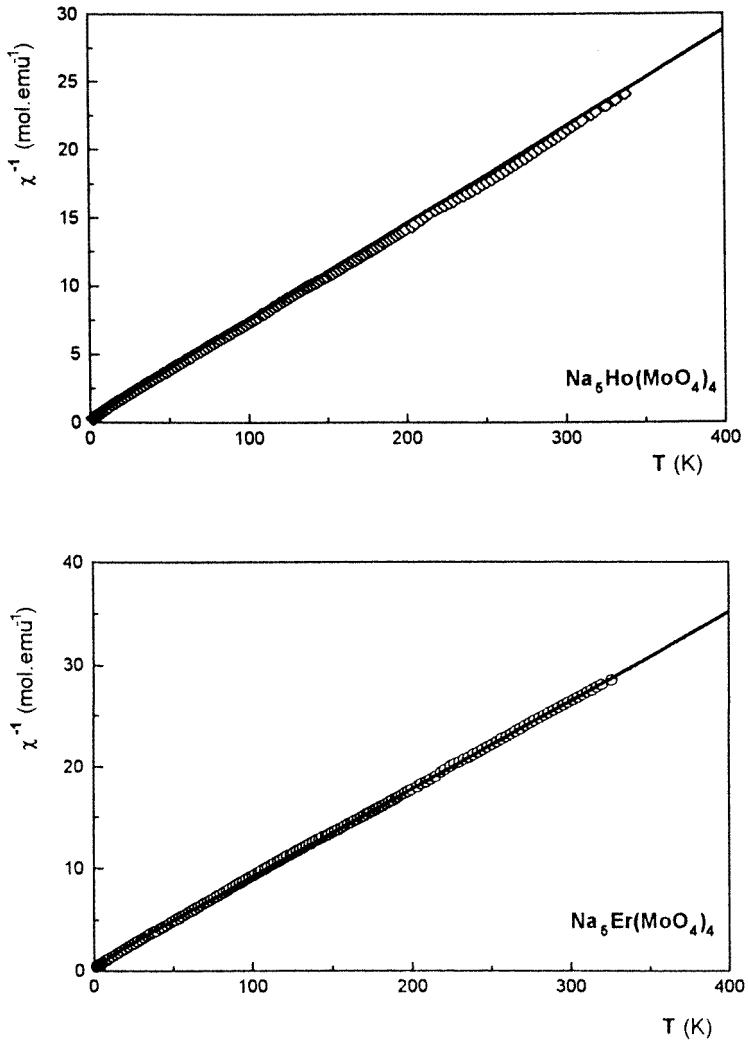

Figure 2. (Continued)

part involving $\varepsilon_1^{(1)}$, i.e., the temperature-dependent term of the susceptibility, is the most important contribution to the paramagnetic susceptibility. In fact, it corresponds to the quantum expression for the Curie–Weiss law. The off-diagonal, temperature-independent terms in the formula, a result of the second-order perturbation, usually have little importance, with the exception of those for the above-mentioned compounds (the ground state $J = 0$ of Eu^{3+} is only some few hundreds of cm^{-1} lower than the next state $J = 1$, so the second-order terms in the formula are unusually important). Since $^7F_0$ is a non-magnetic level, the diagonal part is cancelled at low temperatures when the next higher state $^7F_1$ is not populated, with only the second-order element in the above expression, $\varepsilon_{^7F_0}^{(2)}$, not negligible. Then the non-diagonal interaction is solely responsible for the well-known paramagnetic temperature-independent susceptibility plateau. This underlines the sensitivity

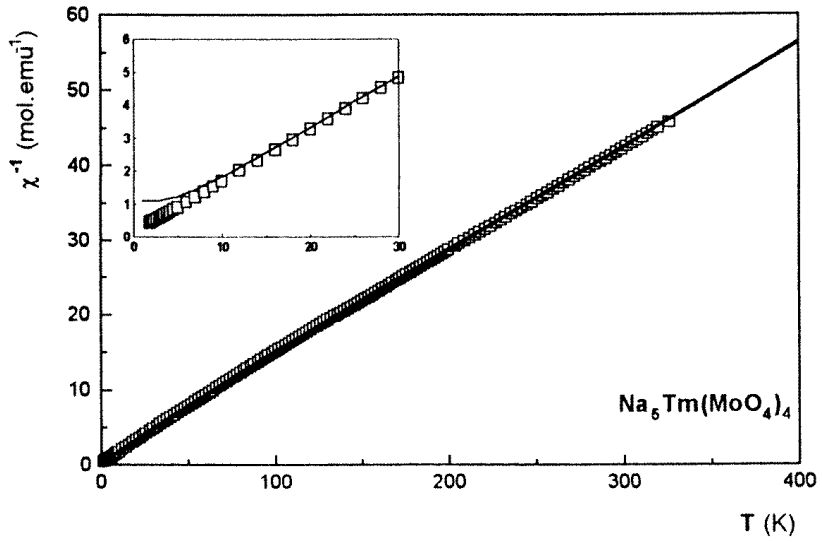

Figure 2. (Continued)

of the paramagnetic susceptibility to the value of this element—which, on the other hand, is strongly dependent on the crystal-field strength.

For $4f^N$ configurations, the calculation of the paramagnetic susceptibility agrees fairly closely with experiment [20–23]. The substantial degree of degeneracy of the $4f^6$ configuration makes the simulation more difficult for the Eu^{3+} compounds. The complete crystal-field calculation would require for a low symmetry to diagonalize a 3003-dimensioned secular determinant, although for the D_{2d} (or S_4) symmetry this would be reduced to four submatrices, about 750×750.

6. Magnetic susceptibility calculations for the $Na_5RE(XO_4)_4$ series

In order to simplify the magnetic susceptibility calculation we assume a D_{2d} point symmetry for the rare earth. Moreover, considering that the cfps do not differ significantly between the europium double molybdate and tungstate [1] we reasonably used for both families a unique set of cfps, those from the molybdate series. Two different collections of phenomenological parameters were used in our calculations: (a) cfps obtained from previous simulations on experimental energy level schemes of Pr, Nd and Eu compounds, and for the remaining configurations those deduced from an extrapolation of the systematic trends identified in the evolution of each parameter (figure 1(a)); and (b) cfps calculated by the simple overlap model, SOM (figure 1(b)). In both cases the free-ion parameters are assumed to be those reported by Carnall *et al* [24], with the exception of those for $4f^2$, $4f^3$ and $4f^6$ configurations, where our experimental free-ion parameters were used [2]. Calculations of the energy levels and magnetic properties of the $4f^N$ configurations were performed using the Fortran computer programs REEL and IMAGE [25].

7. Discussion

Figures 1(a) and 1(b) show the variation of the cfps through the rare-earth series versus the atomic number compared to (a) extrapolated values from experimental data, and to (b) those calculated using the SOM. A major difference is found only for B_0^4, whereas other cfps have comparable orders of magnitude.

Figure 2 presents a comparison between the experimental and calculated magnetic susceptibilities (using the cfps from figure 1(a)) for most of the compounds of the molybdate series. There is almost no difference between molybdate and tungstate compounds for the experimental values, which has to be correlated with the closeness of the optical spectra and justify calculations with the same set of parameters. At high temperatures, the susceptibilities follow a Curie–Weiss-type behaviour. Deviations from linearity observed at low temperature can be attributed to the splitting of the free-ion ground state under the influence of the crystal field, and the Weiss constants for these materials are entirely due to crystal-field effects since they do not undergo any magnetic exchange interactions. The simulation is very good for the whole series except the case of the praseodymium compounds, which has often been found to be the case for different matrices and is discussed elsewhere [23, 26].

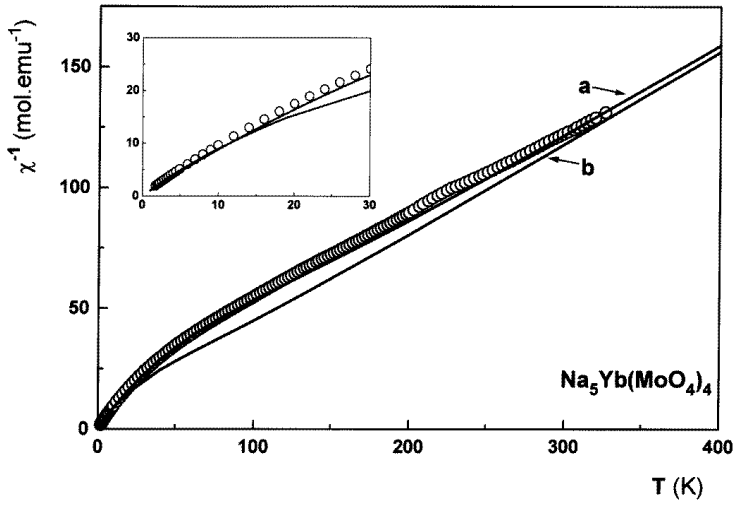

Figure 3. A comparison between experimental (symbol) and calculated (solid lines) reciprocal paramagnetic susceptibility curves for $Na_5Yb(MoO_4)_4$: (a) from extrapolated cfps, figure 1(a); and (b) from cpfs calculated using the SOM, figure 1(b).

This type of simulation offers an excellent opportunity to test the effect of the cfps on paramagnetic susceptibility curves. Except in the case of Eu^{3+} [1] and to a lesser extent the case of Sm^{3+}, for which the non-diagonal term $\varepsilon_i^{(2)}$ has great importance, the curve deviating most strongly from the Curie–Weiss law is found to be that for Yb^{3+}. This is mainly due to the thermal population effect, but also to the particular values of individual matrix elements affected by the cfps values. This ion, located at the end of the rare-earth series, also presents the largest difference between calculated and estimated parameters. This is why the reciprocal susceptibility curves calculated by using both sets of cfps reported on figures 1(a) and 1(b) for $Na_5Yb(MoO_4)_4$ are compared to the experimental results in figure 3. It is clearly shown that the discrepancy is not very important in spite of the large

difference between the two B_0^4-parameters. In fact, for molybdates or tungstates with the remaining, lighter than Yb^{3+}, rare-earth ions, the observed differences between the two calculated susceptibility curves are negligible.

The crystal-field strength appears to be not very sensitive in the paramagnetic susceptibility curves. A good simulation can be considered as a confirmation for obtaining 'good wavefunctions' only through using 'good cfps' such as those that we obtained experimentally for Pr^{3+}, Nd^{3+} and Eu^{3+}, and to a lesser extent, for the other rare-earth ions with extrapolated values. In contrast, it seems to be more difficult to deduce one cfp set from a given susceptibility curve, i.e., susceptibility measurements on polycrystalline powders do not determine the cfps at all accurately, even when the point symmetry is relatively high, except for in special cases for which only some of the cfps are predominant (e.g. the case of the Eu^{3+} plateau position). That means that in the possible case of opaque compounds the approach of the crystal-field strength would require more than the knowledge of the paramagnetic susceptibility. We think that this problem could be solved only if that information is connected with the position of the first crystal-field levels deduced from inelastic neutron scattering or specific heat measurements, and completed with a model for calculating the cfps from the crystallographic positions.

Acknowledgments

The authors acknowledge the financial support of the 'Integrated Action' No 188B, 1995, from the Spanish and French Education and Research Ministries.

References

[1] Huang J, Loriers J Porcher P, Teste de Sagey G, Caro P and Levy-Clement C 1984 *J. Chem. Phys.* **80** 6204
[2] Antic-Fidancev E, Cascales C, Lemaître-Blaise M and Porcher P 1994 *J. Alloys Compounds* **207/208** 178
[3] Baran E J, Vasallo M B, Cascales C and Porcher P 1993 *J. Phys. Chem. Solids* **54** 1005
[4] Mulay L N 1963 *Magnetic Susceptibility* (New York: Wiley) p 1782
[5] Wybourne B G 1965 *Spectroscopic Properties of Rare Earths* (New York: Wiley)
[6] Newmann D J 1971 *Adv. Phys.* **20** 197
[7] Schäffer C E 1972 *Struct. Bonding* **14** 69
[8] Smith D W 1978 *Struct. Bonding* **35** 85
[9] Morrison C A and Leavitt R P 1982 *Handbook on the Physics and Chemistry of Rare Earths* vol 5 (Amsterdam: North-Holland)
[10] Sternheimer R M, Blume M and Peierls R F 1968 *Phys. Rev.* **173** 376
[11] Malta L M 1982 *Chem. Phys. Lett.* **88** 353
[12] Porcher P 1995 The optical spectroscopy of rare earth ions *Summer School of the University Complutense of Madrid: 200 Years of Rare Earths*
[13] Porcher P and Malta O L 1996 *Ab initio* calculation of crystal field parameters: applications of the 'simple overlap model' to rare earth and transition elements compounds *Winter Workshop on Spectroscopy and Structure of Rare Earth Systems (Wroclaw)*
[14] Chang N C, Gruber J B, Leavitt R P and Morrison C A 1982 *J. Chem. Phys.* **76** 3877
[15] Leavitt R P, Morrison C A and Wortman D E 1975 Rare earth ion–host crystal interaction 3. Three-parameters theory of crystal field *Harry Diamond Laboratories Report* TR-1673
[16] Mokhosoev M V, Alekseev F P and Get'man E I 1969 *Zh. Neorg. Khim.* **14** 596
[17] Efremov V E, Berezina T A, Averina I M and Trunov V K 1989 *Kristallografiya* **25** 254
[18] Van Vleck J H 1932 *The Theory of Electric and Magnetic Susceptibilities* (London: Oxford University Press) p 245 ff
[19] Van Vleck J H 1968 *J. Appl. Phys.* **39** 365
[20] Saez-Puche R, Antic-Fidancev E, Lemaître-Blaise M, Porcher P, Cascales C, Marcano C.M and Rasines I 1989 *J. Less-Common Met.* **148** 369

[21] Antic-Fidancev E, Cascales C, Lemaître-Blaise M, Saez-Puche R and Rasines I 1991 *Eur. J. Solid State Inorg. Chem.* **28** 77
[22] Cascales C, Saez-Puche R and Porcher P 1993 *J. Phys. Chem. Solids* **54** 1471
[23] Cascales C, Saez-Puche R and Porcher P 1995 *J. Solid State Chem.* **114** 52
[24] Carnall W T, Goodman G L, Rajnak K and Rana R S 1989 *J. Chem. Phys.* **90** 3443
[25] Porcher P 1989 Fortran routines REEL and IMAGE for simulation of d^N and f^N configurations involving real and complex crystal field parameters, unpublished
[26] Guo M D, Aldred A T and Chan S K 1987 *J. Phys. Chem. Solids* **48** 229